

The Effect of Multi-Stage Constant Current Charging on Lithium-ion Battery's Performance

Tahir, Muhammad Usman; Sangwongwanich, Ariya; Stroe, Daniel-Ioan; Blaabjerg, Frede

Published in:

Proceedings of the 2023 IEEE 17th International Conference on Compatibility, Power Electronics and Power Engineering (CPE-POWERENG)

DOI (link to publication from Publisher):

[10.1109/CPE-POWERENG58103.2023.10227383](https://doi.org/10.1109/CPE-POWERENG58103.2023.10227383)

Publication date:

2023

Document Version

Accepted author manuscript, peer reviewed version

[Link to publication from Aalborg University](#)

Citation for published version (APA):

Tahir, M. U., Sangwongwanich, A., Stroe, D.-I., & Blaabjerg, F. (2023). The Effect of Multi-Stage Constant Current Charging on Lithium-ion Battery's Performance. In *Proceedings of the 2023 IEEE 17th International Conference on Compatibility, Power Electronics and Power Engineering (CPE-POWERENG)* Article 10227383 IEEE (Institute of Electrical and Electronics Engineers). <https://doi.org/10.1109/CPE-POWERENG58103.2023.10227383>

General rights

Copyright and moral rights for the publications made accessible in the public portal are retained by the authors and/or other copyright owners and it is a condition of accessing publications that users recognise and abide by the legal requirements associated with these rights.

- Users may download and print one copy of any publication from the public portal for the purpose of private study or research.
- You may not further distribute the material or use it for any profit-making activity or commercial gain
- You may freely distribute the URL identifying the publication in the public portal -

Take down policy

If you believe that this document breaches copyright please contact us at vbn@aub.aau.dk providing details, and we will remove access to the work immediately and investigate your claim.

The Effect of Multi-Stage Constant Current Charging on Lithium-ion Battery's Performance

Muhammad Usman Tahir
Department of Energy
Aalborg University
Aalborg, Denmark
mut@energy.aau.dk

Ariya Sangwongwanich
Department of Energy
Aalborg University
Aalborg, Denmark
ars@energy.aau.dk

Daniel-Ioan Stroe
Department of Energy
Aalborg University
Aalborg, Denmark
dis@energy.aau.dk

Frede Blaabjerg
Department of Energy
Aalborg University
Aalborg, Denmark
fbl@energy.aau.dk

Abstract— The multi-stage constant current (MSCC) charging strategy is intended to enhance the performance of lithium-ion batteries (LIBs). Therefore, this paper investigates the MSCC charging effect on LIB's performance parameters, including charging time, charged/discharged capacity, charging energy efficiency, and maximum/average temperature rise. A 2.6 Ah lithium-iron-phosphate (LFP)-based Li-ion battery is subjected to a five-stage MSCC charging at different current rates, with SOC-based transition. The impact of the MSCC charging method on the LIB performance parameters is evaluated against the traditional CCCV charging method. The experimental findings demonstrate that the MSCC technique can reduce the charging time by 13.3% while keeping similar charged/discharged capacity and charging energy efficiency as the CCCV method, with a 1.4% reduction in maximum temperature rise at a 3.5 C charging rate. The MSCC charging technique can be useful for fast-charging LIBs in EV applications and other applications that require high charging rates while maintaining safety.

Keywords— *Li-ion battery, Charging Strategies, Multi-stage Constant Current (MSCC), Constant Current – Constant Voltage (CCCV), Charging Time, Temperature Rise.*

I. INTRODUCTION

As electric transportation has been recognized as an essential factor in enhancing urban air quality and decreasing reliance on fossil fuels, various efforts and works are being undertaken in academia and industry to facilitate the global development of electric vehicles (EVs). By the end of the year 2021, there were approximately 16.5 million EVs on roads all over the world [1]. The lithium-ion battery (LIB) is the core technology to power EVs. LIBs are distinguished from lead-acid batteries by their high energy/power density, low self-discharge rate, and long cycle life [2, 3]. In the past decade, range anxiety has been recognized as one of the major impediments to the widespread adoption of EVs. However, nowadays, the primary challenge that needs to be overcome is the charge duration. Charging time at home is substantially longer (8-10 hours) than commercial (2-6 hours) and fast chargers (15 to 60 minutes); the charging time depends on the charger manufacturer and the power rating of the charger. However, the primary risk of fast charging is the rising battery temperature during charging. Due to the high current in fast chargers, the temperature rises, which is detrimental to the battery's health. Moreover, thermal runaways and battery explosions also have significant concerns about safety issues. Therefore, this paper focuses on assessing the fast-charging technique considering the charging time and thermal behavior of LIBs.

During charging, either the battery's power, current, or voltage are regulated depending on the charging method. The constant current constant voltage (CCCV) charging method is

widely applied for all LIBs [4]. The CCCV charging has two modes: constant current (CC) mode and constant voltage (CV) mode. First, LIB is charged with constant current (I_{chg}) in CC mode until the LIB voltage reaches the cut-off voltage (V_{max}), and in the second mode, the voltage is kept constant at (V_{max}) until the current drops below 5% of the current (I_{end}) corresponding to the nominal battery capacity. The charging time is mainly related to the charging current (C-rate) of CC mode, while the CV mode facilitates the LIB to obtain a higher charged capacity, but it increases the charging time. The manufacturer usually defines the I_{chg} rating, which depends on the LIB's chemistry. Furthermore, high C-rates have a negative effect on LIB's health. On the other hand, CV mode generally takes a longer charging time and only has a limited contribution to the amount of charged capacity [4].

Several charging techniques were proposed and investigated in the literature to improve LIB's charging performance. Boost charging (BC) was developed to reduce the charging time while retaining the available capacity and cycle life of LIBs [5]. In [6], the sinusoidal ripple current (SRC) is proposed and tested to improve the charging efficiency, shorten the charging time, reduce maximum rising temperature, and improve LIB's lifetime by about 1.9%, 17%, 45.8%, and 16.1%, respectively. In [7], the effect of the positive pulse current (PPC) on the performance of LIBs is investigated, and the result demonstrates that PPC can extend the LIB lifetime by 60% at low frequency (0.05 Hz) and by 105% at high frequency (2 kHz). The Taguchi orthogonal arrays technique was used in [8] to find the optimal pulse charging parameters that improve LIB charge and energy efficiency while reducing charging time. It was discovered that operating a PPC with ideal parameters reduced charge time by 47.6 % and enhanced LIB charge and energy efficiency by 1.5% and 11.3%, respectively. The multi-stage constant current (MSCC) charging strategy has been proposed to shorten the charging time, improve the charging and discharging capacity, reduce the temperature rise, and prolong the lifetime of LIBs [9-15]. There are three important parameters when implementing the MSCC: 1) the number of stages, 2) transition criteria from one stage to another 3) the charging current (C-rate) for each stage. In [16], the effect of the number of stages on the MSCC charging strategy has been analyzed. It concluded that as the number of stages increases from one to five, the charging time is reduced. However, only marginal improvements can be achieved above the five stages.

Furthermore, four different transition criteria can be applied to move from one stage to another: time-based transition [14], cut-off voltage-based transition [10], SOC-based transition [9], and threshold voltage-based transition [15]. In the literature, most researchers used the cut-off voltage-based transition and SOC-based transition. In [17],

TABLE I. THE EXISTING RESEARCH PAPERS ON THE MULTI-STAGE CONSTANT CURRENT (MSCC) WITH SOC-BASED TRANSITION AND ITS IMPACT ON THE PERFORMANCE PARAMETERS

Reference	No. of stages	Max. C-rate	Charging time	Charged Capacity	Studied Performance Parameters			
					Discharged Capacity	Charging/Energy Efficiency	Max Temperature Rise	Average Temperature Rise
[9]	2,3,4	2	✓	✓	✓	×	✓	×
[17]	4	1.5	✓	✓	✓	✓	×	×
[16]	4,5,10,20	1	✓	×	×	✓	×	×
[18]	8	5	✓	×	×	×	✓	×
[19]	4	2	✓	✓	✓	✓	✓	×
This work	5	3.5	✓	✓	✓	✓	✓	✓

the effect of the four-stage charging with SOC-based transition on the LIB charging time, charged and discharged capacity, and charging efficiency was analyzed. The results showed that the four-stage charging with SOC-based transition charged the LIB 30 minutes faster than the 0.7 C-rate of CCCV charging. In [18], the SOC-based transition is used for eight-stage MSCC to balance the charging time and temperature rise during the charging. However, the impact of the MSCC on the entire range of C-rates is not investigated yet. Table I presents the existing research articles based on SOC transition and their impact on the performance parameters. Therefore, the impact of the MSCC in a broader spectrum of C-rates with SOC transition should be explored and compared with the corresponding CCCV technique in order to find performance parameters. Additionally, the previous research did not consider the impact of MSCC on the average temperature rise, which is a crucial parameter for the safety and performance-degradation behavior of LIBs.

This paper investigates the effect of the MSCC charging on the charging and discharging capacity, charging energy efficiency, charging time, and thermal behavior (including average temperature rise and maximum temperature rise) of the lithium iron phosphate (LFP) battery. The LFP battery cell was tested considering different C-rates at 25°C and compared with the equivalent CCCV method. The remaining sections of the paper are organized as follows. Section II considered the experimental setup with an introduction of MSCC and performance parameters and their definitions. Section III discussed the MSCC effect on the performance parameters and compared it with the CCCV method. Section IV represents the quantitative analysis based on the fitted equations. Section V concludes the key findings of the paper.

II. EXPERIMENTAL SETUP

A. MSCC Charging Strategy

This paper investigates the five-stage constant current charging technique with SOC-based transition. Fig. 1 shows a generalized MSCC waveform with a SOC-based transition. The charging current is shown as I_1, I_2, \dots, I_n , while the associated SOC stages are shown as $SOC_1, SOC_2, \dots, SOC_n$.

B. LFP Cell

The key characteristics of the used LFP cell are summarized in Table II. The Neware battery testing station is used for all experiments. The cell is placed in the Memmert temperature chamber to maintain a constant and reliable temperature during experimentation, as illustrated in Fig. 2.

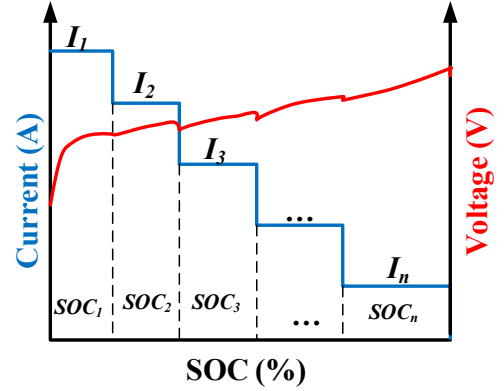


Fig. 1. An example of a Multi-Stage Constant Current (MSCC) charging waveforms with SOC-based transition (blue: current, red: voltage)

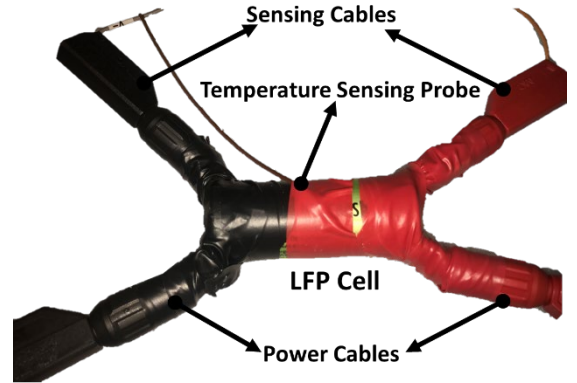


Fig. 2. LFP Cell in temperature chamber during testing

TABLE II. KEY CHARACTERISTICS OF THE TESTED LFP BATTERY CELL

Characteristic	Value
Nominal capacity (Ah)	2.6
Nominal voltage (V)	3.3
Cut-off voltage (V)	3.6
Minimum discharge voltage (V)	2
Maximum charge current (A)	10.4
Operating temperature (°C)	-30 – 55
Internal Impedance (1 kHz typical)	6 mΩ

C. Test Procedure

The LFP cell was charged at 25°C using a five-stage MSCC charging strategy, and the traditional CCCV method was used for benchmarking. At a low SOC level, a high charging rate will not lead to the deterioration of the cell's electrode materials [14]. Therefore, the SOC interval for the first stage is set to 0-50% with the highest C-rate level. The LIB is charged within 50-70% of the SOC in the second stage, and the remaining 30% of SOC is charged in three stages with 10% of SOC intervals. All experiments are carried out in accordance with the specified SOC level. The impact of MSCC on LIB performance is analyzed. The following is the testing procedure for MSCC:

1. Tempering the LIB at 25°C for 1 hour.
2. Discharge the LIB at 1C current until the discharge cut-off voltage (2V) is reached.
3. Relaxation of the LIB at 25°C for one hour to stabilize the open circuit voltage (OCV) and thermal stress
4. Charge the LIB at a particular C-rate for each stage until the SOC interval or 3.6V is reached.
5. Relaxation of the LIB at 25°C for 1 hour if the average C-rate is less than 1C; otherwise, 1.5 hours of relaxation is applied to stabilize the OCV and thermal stress.
6. Discharge the LIB at 1C current until the discharge cut-off voltage (2V) is reached.
7. Relaxation of the LIB at 25°C for one hour to stabilize the OCV and thermal stress
8. Repeat steps 4-7 for all experiments

The same LIB cell is charged using the CCCV method at 0.6C, 1C, 1.5C, 2C, 2.5C, 3C, and 3.5C at a temperature of 25°C for comparison. Every experiment's discharge stage was conducted at 1C to ensure a fair comparison.

Fig. 3(a) shows an example of the measured current, voltage, and temperature signals during the five-stage MSCC charging strategy. Fig. 3(b) shows an example of the measured current, voltage, and temperature during CCCV charging.

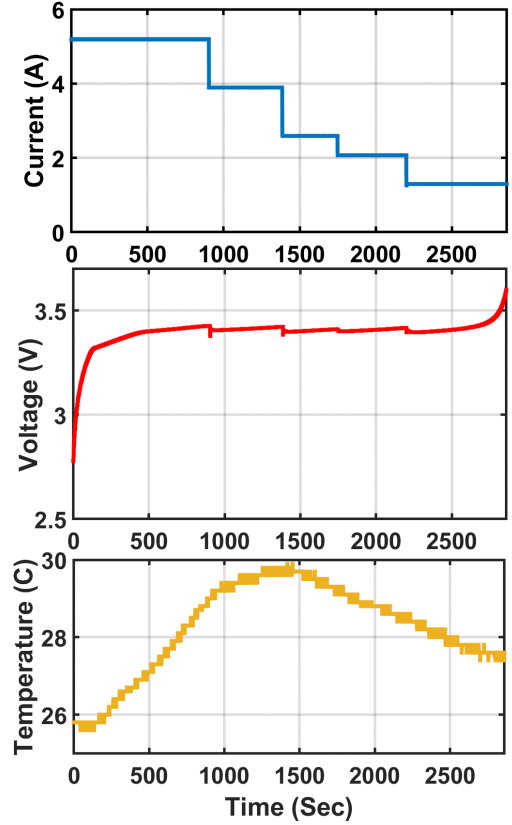
III. MODELING AND DISCUSSION

The LIB is charged and discharged in accordance with the aforementioned test procedure in order to determine the impact of the MSCC charging strategy on the performance parameters. Therefore, several experiments are carried out at varying average C-rates. Average C-rate means: the sum of all the current divided by total time as given in (1).

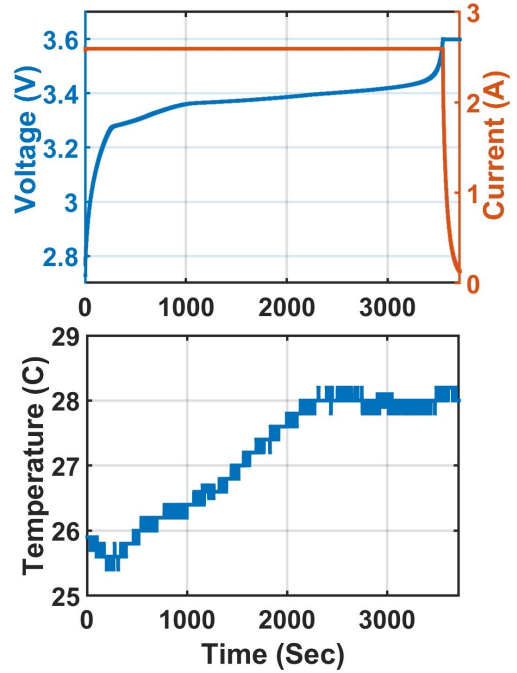
$$C_{avg} = \frac{\sum_{j=1}^5 I_j}{T} \quad (1)$$

Where C_{avg} represents MSCC's average current. T is the total charging time, while J denotes the number of stages.

Table III summarizes the experiments and effects of the MSCC charging strategy on key performance parameters compared to the CCCV method. Based on the conducted experiments, the interpolation of the charging time, maximum temperature rise, and C-rate is shown in Fig. 4 for both MSCC and CCCV methods. The effect of the MSCC on the performance parameters is examined in more detail below.



(a)



(b)

Fig. 3. Examples of the MSCC charging and CCCV charging strategies a) a five-stage MSCC charging strategy with an average C-rate of 1.25C b) a CCCV charging voltage, current, and temperature plots at 1 C-rate

A. Charging Time

The effect of the MSCC on the charging time can be analyzed in Table III. MSCC charging strategy takes less time to charge a LIB than the equivalent CCCV method, as shown in Fig. 5(a). In the SOC-based transition criterion, first and

TABLE III. SUMMARY OF THE CONDUCTED EXPERIMENTS AND THEIR IMPACT ON THE PERFORMANCE PARAMETERS

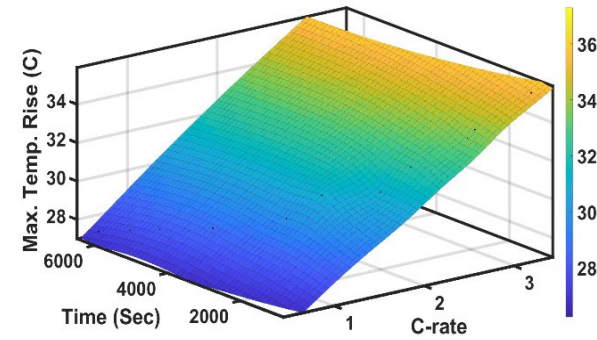
Experiment Number	Charging Strategy	C-rate	Studied Performance Parameters					
			Charging Time (s)	Charged Capacity (Ah)	Discharged Capacity (Ah)	Energy Efficiency (%)	Max. Temperature Rise (°C)	Average Temperature Rise (°C)
1	MSCC	0.574	6221	2.58	2.61	96.4	27.4	26.5
2		0.644	5522	2.57	2.61	96.3	27.9	26.8
3		0.725	4911	2.57	2.61	96.2	28.3	27
4		0.91	3917	2.58	2.61	95.8	28.9	27.5
5		1.25	2734	2.58	2.60	95.1	29.9	28.2
6		1.50	2385	2.59	2.60	94.5	31.1	29.1
7		1.93	1837	2.57	2.59	94.1	31.2	29.4
8		2.18	1630	2.57	2.59	93.7	32.4	30.2
9		2.69	1308	2.55	2.56	93.3	33.6	30.3
10		2.76	1284	2.56	2.58	93.1	34	31.2
11		3.30	1069	2.56	2.56	92.1	35.5	31.9
12	CCCV	0.6	6060	2.57	2.61	96.9	27.2	26.5
13		0.8	4595	2.58	2.61	96.2	27.7	26.9
14		1.0	3713	2.58	2.61	95.9	28.2	27.2
15		1.5	2537	2.59	2.61	94.9	29.9	28
16		2.0	1939	2.59	2.61	94.1	31.6	29
17		2.5	1575	2.59	2.61	93.6	33.5	29.8
18		3.0	1330	2.59	2.61	93	35.1	30.8
19		3.5	1153	2.59	2.61	92.4	36.8	31.7

second-stage currents in MSCC have a higher C-rate than the constant current (I_{chg}) in the CCCV method. As a result, the charge time is shorter in the first half of the charging period. Furthermore, the second half takes longer to charge the same capacity due to the lower charging C-rate. The overall charging time in the MSCC is shorter than the equivalent CCCV charging time; nevertheless, the obtained difference is marginal.

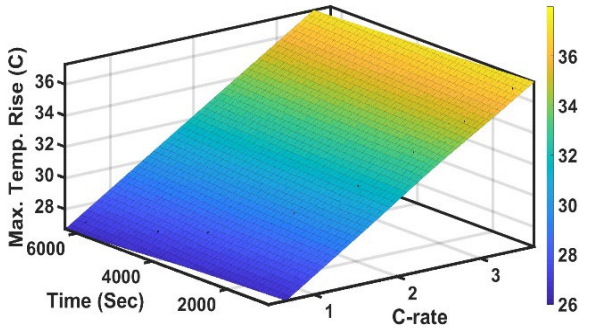
However, the data points of MSCC charging time are not aligned with the CCCV data points. So, the corresponding data points can be obtained using interpolation instead of more experimentation. The MATLAB curve fitting tool application is used to find the fitted line equation, as shown in Fig. 5(b). Equation (2) describes the relationship between the charging time and the average C-rate with R^2 of 0.9997.

$$Chg_{time} = 3545C^{-1.01} \quad (2)$$

Where C is the average C-rate of the MSCC charging strategy, the charging time is reduced with the increase of the average C-rate as shown in Fig. 5(a).

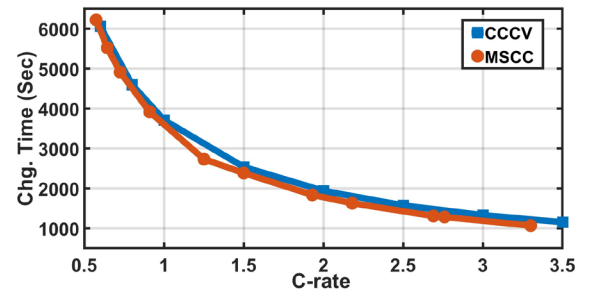


(a)

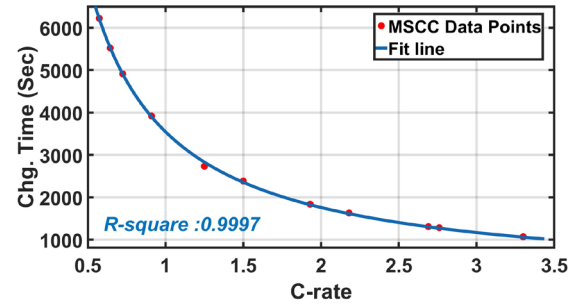


(b)

Fig. 4. Determined and the fitted charging time and Max. Temperature based on the C-rate a) For MSCC Charging Strategy b) For CCCV charging



(a)



(b)

Fig. 5. The effect of the C-rate on MSCC and CCCV charging time a) Comparison between MSCC and CCCV b) Fitted line for MSCC charging time

B. Charged and Discharged Capacity

The MSCC's impact on both charging and discharging capacity is illustrated in Table III. At the higher C-rate (3.3C), above 98% of the capacity is charged and discharged. Therefore, the LIB is nearly fully charged utilizing the MSCC charging technique. The MSCC charging strategy involves a high C-rate in the initial stages and a gradual decrease in the C-rate in five stages. On the other hand, the CCCV charging strategy gradually decreases the C-rate throughout the CV mode. In most cases, the CCCV method tends to have a slightly higher charged/discharged capacity compared to MSCC.

However, below 1.5 C-rate, there is no significant difference between the charged and discharged capacities of the LIB using MSCC and CCCV. This is because the charging rate is low, and the heat generated is minimal, resulting in little to no impact on the battery's capacity.

C. Charging Energy efficiency

The charging energy efficiency is the ratio of the totally discharged energy from the LIB to the total charged energy into the LIB during one whole cycle, as shown in (3).

$$\eta_{chg} = \frac{\text{Dis. Chg. Energy (Wh)}}{\text{Chg. Energy (Wh)}} = \frac{\int_0^t P_d \cdot dt}{\int_0^t P_c \cdot dt} \quad (3)$$

The impact of the MSCC on the LIB's energy efficiency is shown in Table III. The charging energy efficiency of the CCCV method is slightly higher than the MSCC method, as shown in Fig. 6. The graph demonstrates that the CCCV is slightly more efficient at higher C rates. The differences in efficiency between the two methods are small, typically not exceeding 0.3%.

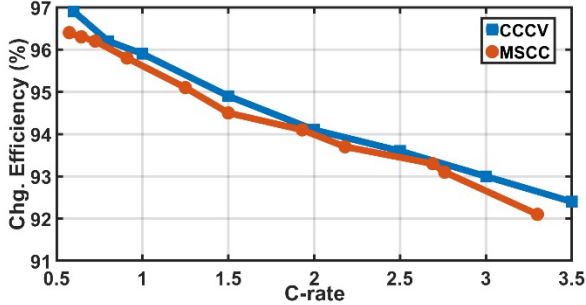


Fig. 6. The effect of MSCC and CCCV on the charging energy efficiency

D. Thermal Behavior (Max. temperature and average temperature)

The effect of MSCC charging on maximum and average temperature rise is depicted in Fig. 7 (a). According to the results of the experiments, the impact of the MSCC charging strategy on the maximum temperature rise at a higher C-rate (2.5 C) is slightly lower than that of the corresponding CCCV method. However, at lower C-rates (below 2C), MSCC has a slightly higher maximum temperature rise than the equivalent CCCV charging method. The heat generated by the LIBs generally increases as the C-rate increases during charging. When the C-rate is high, more energy goes into the battery in a shorter period of time, which can increase the battery's internal resistance and cause it to produce more heat. This heat can cause the battery's temperature to increase, resulting in a decline in performance and a shorter lifespan. In the case of MSCC, the charging current is high in the initial stages, which can cause the internal resistance of the battery to increase and

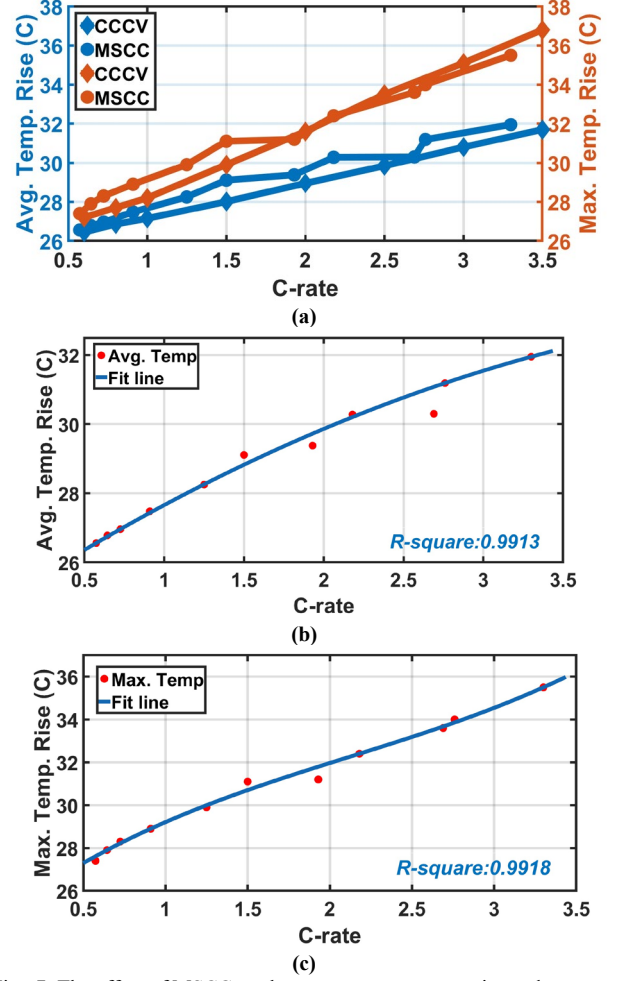


Fig. 7. The effect of MSCC on the average temperature rise and max. temperature rise during charging a) showing the fitted line of Average temperature rise against C-rate b) showing the fitted line of max. temperature rise against C-rate

generate more heat. As the charging rate is reduced in later stages, the temperature rise slows down. On the other hand, in the CCCV method, the charging current is constant throughout the charging process, and the heat generated during charging is gradually increased. Thus, at the higher C-rate, MSCC has a low-temperature rise compared to the equivalent CCCV method.

Furthermore, the MSCC charging strategy affects average temperature rise slightly more than the CCCV method. The temperature rises faster in the first and second stages of MSCC than in the CCCV method. Overall, the average temperature is likely to be higher in MSCC than in the CCCV method.

The average temperature rise and maximum temperature rise against C-rate are fitted with a suitable polynomial with R^2 of 0.99 to do the quantitative analysis, as illustrated in Figs. 7 (b) and 7 (c). Equations (4-5) depict the equations of the fitted lines.

$$T_{avg} = -0.26C^2 + 2.98C + 24.93 \quad (4)$$

$$T_{max} = 0.25C^3 - 1.58C^2 + 5.76C + 24.78 \quad (5)$$

IV. QUANTITATIVE ANALYSIS

The effects of the MSCC on the charging capacity, discharging capacity, and charging energy efficiency are excluded from the quantitative analysis because of the insignificance of the variations between MSCC and CCCV

charging methods. However, the charging time and thermal behavior must be discussed and evaluated using experimental data. Table IV presents the fitted values for several performance parameters at the corresponding values of CCCV. Compared to the equivalent CCCV charging technique, the charging time is reduced by 9.2% at 2C charging current, with a maximum temperature drop of 2.9% and 1.2% in average temperature. As a result of its lower maximum temperature rise and shorter charging time, MSCC charging can be used for fast charging of an EV and other applications where higher charging rates are required. It's worth noting that the above observations are based on a specific experimental setup, and the result may change depending on the battery's design and charging condition.

TABLE IV. QUANTITATIVE ANALYSIS BETWEEN MSCC AND CCCV CHARGING METHOD

Charging Strategy	C-rate	Charging Time (s)	Max. Temperature Rise (°C)	Average Temperature Rise (°C)
MSCC	1	3545	29.21	27.65
	2	1760	31.98	29.85
	3	1167	34.59	31.53
	3.5	1000	36.30	32.17
CCCV	1	3717	28.2	27.2
	2	1939	31.6	29.0
	3	1330	35.1	30.8
	3.5	1153	36.8	31.7

V. CONCLUSION

This paper investigates the effect of MSCC charging on LIB performance in terms of charging time, charged/discharged capacity, charging energy efficiency, and the maximum/average temperature rise. The SOC-based stage transition criterion is used for stage transitions from one to another. On the LFP cell, a five-stage constant current charging is applied to charge the battery at several average C-rates ranging from 0.57 C to 3.3 C. In order to compare with MSCC, the LFP cell is charged by employing the CCCV charging method at various C-rates. The results indicate that MSCC has no significant effect on the charged/discharged capacity and charging energy efficiency compared to CCCV. However, the primary effects of MSCC can be observed in the charging time and maximum and average temperature rise during charging. For quantitative analysis, the modeling of performance parameters has been done to determine the key points (charging time, maximum temperature rise, and average temperature rise) of MSCC against CCCV. The charging time can be shortened by 13.3% when compared to the equivalent CCCV, with a 1.4% decrease in maximum temperature rise at a 3.5 C rate. Generally, the health of LIBs and safety during operations can be improved by lowering the maximum temperature rise during charging. The MSCC charging technique can be used to fast-charge LIBs for EV applications and other applications that require high charging rates while maintaining safety.

For future work, the LFP battery will be examined at varying thermal conditions with a cut-off voltage transition. Additionally, a variable number of stages will be investigated by employing the MSCC strategy for a wide range of experiments for comparison with the CCCV technique.

REFERENCES

- [1] IEA, "Global EV Outlook 2022," IEA., 2022. <https://www.iea.org/reports/global-ev-outlook-2022>.
- [2] M.U. Tahir, M. Anees, H.A. Khan, I. Khan, N. Zaffar and T. Moaz, "Modeling and evaluation of nickel manganese cobalt based Li-ion storage for stationary applications," *Journal of Energy Storage*, vol. 36, pp. 102346, 2021.
- [3] M. U. Tahir, T. Moaz, H. A. Khan, N. A. Zaffar and I. Khan, "Accurate Modeling of Li-ion Cells Applied to LiFePO₄ and NMC Chemistries," - 2020 *IEEE Texas Power and Energy Conference (TPEC)*, pp. 1-6, 2020.
- [4] X. Huang, W. Liu, A.B. Acharya, J. Meng, R. Teodorescu and D. Stroe, "Effect of pulsed current on charging performance of lithium-ion batteries," *IEEE Trans.Ind.Electron.*, vol. 69, pp. 10144-10153, 2021.
- [5] P. Keil and A. Jossen, "Charging protocols for lithium-ion batteries and their impact on cycle life—An experimental study with different 18650 high-power cells," *Journal of Energy Storage*, vol. 6, pp. 125-141, 2016.
- [6] L. Chen, S. Wu, D. Shieh and T. Chen, "Sinusoidal-ripple-current charging strategy and optimal charging frequency study for Li-ion batteries," *IEEE Trans.Ind.Electron.*, vol. 60, pp. 88-97, 2012.
- [7] X. Huang, "The Effects of Pulsed Charging Current on the Performance and Lifetime of Lithium-Ion Batteries," 2021.
- [8] J.M. Amanor-Boadu, A. Guiseppi-Elie and E. Sánchez-Sinencio, "Search for optimal pulse charging parameters for Li-ion polymer batteries using Taguchi orthogonal arrays," *IEEE Trans.Ind.Electron.*, vol. 65, pp. 8982-8992, 2018.
- [9] D. Ji, L. Chen, T. Ma, J. Wang, S. Liu, X. Ma and F. Wang, "Research on adaptability of charging strategy for electric vehicle power battery," *J.Power Sources*, vol. 437, pp. 226911, 2019.
- [10] G. Chen, Y. Liu, S. Wang, Y. Luo and Z. Yang, "Searching for the optimal current pattern based on grey wolf optimizer and equivalent circuit model of Li-ion batteries," *Journal of Energy Storage*, vol. 33, pp. 101933, 2021.
- [11] P. Makeen, H.A. Ghali and S. Memon, "A Review of Various Fast Charging Power and Thermal Protocols for Electric Vehicles Represented by Lithium-Ion Battery Systems," *Future Transportation*, vol. 2, pp. 15, 2022.
- [12] Y. Zhang, S. Xu and T. Wu, "Multi-stage constant current charging strategy considering SOC intervals and voltage thresholds," *Global Energy Interconnection*, vol. 5, pp. 143-153, 2022.
- [13] X. Wu, Y. Xia, J. Du, X. Gao and S. Nikolay, "Multi-Stage Constant Current Charging Strategy Based on Multi-Objective Current Optimization," *IEEE Transactions on Transportation Electrification*, 2022.
- [14] F. An, R. Zhang, Z. Wei and P. Li, "Multi-stage constant-current charging protocol for a high-energy-density pouch cell based on a 622NCM/graphite system," *RSC Advances*, vol. 9, pp. 21498-21506, 2019.
- [15] R. Mathieu, O. Briat, P. Gyan and J. Vinassa, "Fast charging for electric vehicles applications: Numerical optimization of a multi-stage charging protocol for lithium-ion battery and impact on cycle life," *Journal of Energy Storage*, vol. 40, pp. 102756, 2021.
- [16] L. Dung and J. Yen, "ILP-based algorithm for Lithium-ion battery charging profile," 2010 *IEEE International Symposium on Industrial Electronics*, pp. 2286-2291, 2010.
- [17] C. Lee, M. Chen, S. Hsu and J. Jiang, "Implementation of an SOC-based four-stage constant current charger for Li-ion batteries," *Journal of Energy Storage*, vol. 18, pp. 528-537, 2018.
- [18] J. Sun, Q. Ma, R. Liu, T. Wang and C. Tang, "A novel multiobjective charging optimization method of power lithium-ion batteries based on charging time and temperature rise," *Int.J.Energy Res.*, vol. 43, pp. 7672-7681, 2019.
- [19] T.T. Vo, X. Chen, W. Shen and A. Kapoor, "New charging strategy for lithium-ion batteries based on the integration of Taguchi method and state of charge estimation," *J.Power Sources*, vol. 273, pp. 413-422, 2015.